Low-lying magnetic excitations of doubly-closed-shell nuclei and nucleon-nucleon effective interactions

V. De Donno, G. Co' and C. Maieron
Dipartimento di Fisica, Università del Salento and,
INFN Sezione di Lecce, Via Arnesano, I-73100 Lecce, ITALY

M. Anguiano, A.M. Lallena and M. Moreno Torres
Departamento de Física Atómica, Molecular y Nuclear,
Universidad de Granada, E-18071 Granada, SPAIN
(Dated: 16th January 2009)

We studied the low lying magnetic spectra of ^{12}C, ^{16}O, ^{40}Ca, ^{48}Ca and ^{208}Pb nuclei within the Random Phase Approximation (RPA) theory. The description of low-lying magnetic states of doubly-closed-shell nuclei imposes severe constraints on the spin and tensor terms of the nucleon-nucleon effective interaction. We have first made an investigation by using four phenomenological effective interactions and we have obtained good agreement with the experimental magnetic spectra, and with the electron scattering responses. Then we made self-consistent RPA calculations to test the validity of the finite-range D1 Gogny interaction. For all the nuclei investigated we have found that this interaction inverts the energies of all the magnetic states forming isospin doublets.

PACS numbers:

I. INTRODUCTION

In the last thirty years, electron scattering experiments on nuclei have produced an enormous amount of high-precision, accurate and reliable data which impose severe constraints on nuclear models and theories. Our interest here is addressed to the excitation of unnatural parity states in the low-lying region of the nuclear spectrum where many responses of several nuclei have been measured [1–10].

The description of these unnatural parity states with effective theories, such as the Random Phase Approximation (RPA), indicates a strong sensitivity to the details of the spin and tensor dependent terms of the Nucleon-Nucleon (NN) effective interactions. While the study of a single excited state, or of a limited set of excited states, for a single nucleus has been pursued in depth, as for example in Refs. [11–13], a systematic study of a large set of nuclei and of excited states has not been presented, and the availability of many precise experimental data has not been fully exploited.

We present here results of such a systematic study which indicates that there are general requirements that the NN effective interaction has to respect in order to provide a reasonable description of the low-lying magnetic excitations. We have obtained these results by using a phenomenological approach to the RPA theory inspired to the Landau-Migdal theory of finite Fermi systems [14, 15]. In this approach the Mean-Field (MF) basis, providing the set of single particle energies and wave functions, is generated by using a Woods-Saxon well, whose parameters are adjusted to reproduce at best some ground state properties of the nucleus, such as the charge density distribution and the single particle energies around the Fermi surface. In addition, a phenomenological residual NN effective interaction is used. The parameters of this interaction are chosen to reproduce the energy of some specific excited state. In terms of comparison with the experimental data, this phenomenological approach uses the RPA theory at its best. In order to study the sensitivity of our results to the details of the residual interaction, we have constructed four phenomenological interactions, two of them of zero-range type, as in the original formulation of the Landau-Midgal theory, and the other two of finite-range type. For each type of interaction we have considered a parameterization with and without tensor terms. We have used these interactions to study the excitation of the low-lying magnetic spectra of ^{12}C, ^{16}O, ^{40}Ca, ^{48}Ca and ^{208}Pb nuclei. We have found only few cases that are sensitive to the differences between the various interactions, and we present them in the paper. The main result of our study is, however, that the major part of the states are equally well described by all the four interactions we have constructed. We have interpreted this results as if we have been able to include some general feature of the interaction necessary to describe well the magnetic excitation spectra of doubly-closed-shell nuclei.

In order to verify this hypothesis, in a second step of our study, we have made RPA calculations within a fully self-consistent approach. This means that the MF states and energies are obtained from a Hartree-Fock (HF) calculation with the same NN effective interaction used in the RPA calculations. In these calculations we have used the Gogny D1 finite-range interaction [16–18]. We have found in this case remarkable disagreements with the experimental data. The most striking result is that all the energies of the states which form an isospin doublet are inverted. This indicates that the good results obtained with the phenomenological approach are not accidental, and that the study of the magnetic spectra is selective in choosing the strength of the relevant terms of the force.

The paper is organized as follows. In Sec. II we give some detail of our calculations, mainly regarding the input used to solve the RPA equations. The results of our study of several magnetic states for all the nuclei under investigation, conducted with the phenomenological approach, are shown in Sec. III. In Sec. IV we present the results of the self-consistent calculation done with the Gogny D1 interaction, for some selected cases. Finally, in Sec. V, we draw our conclusions.

II. DETAILS OF THE CALCULATION

The first input required by the RPA calculation is the set of single particle wave functions and energies. In the phenomenological calculations we used the single particle bases generated by Woods-Saxon wells. The parameters of the wells have been taken from the literature [19], and have been chosen to describe at best the energies of the single particle states around the Fermi surface and the ground state charge density distributions. In the self-consistent calculations, the single particle wave functions and energies have been obtained by solving the Hartree-Fock equations with the method described in Refs. [20, 21].

We solve the RPA equations by using a discrete set of single particle wave functions and energies. In the phenomenological calculations, the discretization of the continuum is obtained by diagonalizing the Woods-Saxon well in a harmonic oscillator basis. In the self-consistent calculations the discretization is obtained by imposing, at the edge of the computing box, to the single particle wave functions the correct boundary conditions of a bound state. The global RPA solutions strongly depend on the size of the single particle configuration space [22]. However, there are excited states dominated by particle-hole excitations where the particle wave function is bound. In this article we consider only this type of states. For each nucleus considered, we have used single particle configuration spaces large enough to ensure the stability of the results for the states under investigation. In the phenomenological calculation the smallest configuration space, used for ^{12}C, is composed of 5 major harmonic oscillator shells, for a total of 44 single particle states. The largest space has been used for ^{208}Pb, and it is composed by 9 major shells for protons and 10 major shells for neutrons, for a total of 100 single particle states. In the self-consistent calculations we have fixed the size of the computational box, $R_{\rm max}$, and the maximum energy of the particle states in the configuration space, $E_{\rm cut}$. In the case of ^{12}C, $R_{\rm max} = 10$ fm and $E_{\rm cut} = 50$ MeV, while for ^{208}Pb these two parameters are 14 fm and 50 MeV, respectively.

The second input required by the RPA is the residual interaction, which, in analogy to the microscopic nucleon-nucleon (NN) interactions of Urbana or Argonne type, we write as

$$\begin{aligned} V_{\rm eff}(1,2) \;=\; & v_1(r_{12}) \,+\, v_1^\rho(r_{12})\,\rho^\alpha(r_1,r_2) \\ & +\, [v_2(r_{12}) \,+\, v_2^\rho(r_{12})\,\rho^\alpha(r_1,r_2)]\;\boldsymbol{\tau}(1)\cdot\boldsymbol{\tau}(2) \\ & +\, v_3(r_{12})\,\boldsymbol{\sigma}(1)\cdot\boldsymbol{\sigma}(2) \,+\, v_4(r_{12})\,\boldsymbol{\sigma}(1)\cdot\boldsymbol{\sigma}(2)\,\boldsymbol{\tau}(1)\cdot\boldsymbol{\tau}(2) \\ & +\, v_5(r_{12})\,S_{12}(\hat{r}_{12}) \,+\, v_6(r_{12})\,S_{12}(\hat{r}_{12})\,\boldsymbol{\tau}(1)\cdot\boldsymbol{\tau}(2)\,, \end{aligned} \tag{1}$$

where, following the indications of past phenomenological [15] and self-consistent [17] RPA studies, we have already considered that both the central and isospin channels depend on the nuclear one-body density $\rho(r)$. In this equation, $r_{12} = |\boldsymbol{r}_1 - \boldsymbol{r}_2|$, $\boldsymbol{\sigma}$ and $\boldsymbol{\tau}$ are the usual spin and isospin operators, S_{12} is the tensor operator defined as

$$S_{12}(\hat{r}) \;=\; 3\,\boldsymbol{\sigma}(1)\cdot\hat{r}\,\boldsymbol{\sigma}(2)\cdot\hat{r} \;-\; \boldsymbol{\sigma}(1)\cdot\boldsymbol{\sigma}(2) \tag{2}$$

and

$$\rho(r_1,r_2) \;=\; [\rho(r_1)\rho(r_2)]^{1/2}\,. \tag{3}$$

The $v_i(r)$ functions of Eq. (1) are the same for all nuclei under investigation. On the other hand, the $v_i^\rho(r)$ corresponding to the density dependent part of the interaction are taken to be different for each nucleus. These density dependent terms are chosen to reproduce the first 2^+ state in ^{12}C and the first 3^- state in ^{16}O, ^{40}Ca, and ^{208}Pb. The other terms of the force are chosen to get a reasonable description of the centroid energy of the isovector giant dipole resonance by caring that the isoscalar spurious 1^- excitation is at zero energy or below. These criteria

are useful for the scalar and isospin terms of the interaction, the main responsible for the excitation of natural parity states. The $v_i(r)$ functions of the spin, spin-isospin and tensor channels of the interaction (i =3,4,5 and 6) are adjusted to describe the excitation energies of the magnetic states below 8 MeV in ^{208}Pb, paying particular attention to the 1^+ states at 5.85 and 7.30 MeV [23], and to the 12^- states at 6.43 and 7.08 MeV [3]. In addition, we also cared to obtain the correct sequence of the two 1^+ states in ^{12}C forming an isospin doublet [2], and that the energy of the first 4^- state of ^{16}O [9] is reasonably reproduced.

In this work we are interested in the possible effects of the tensor channels of the interaction as well as in the relevance of its range (zero or finite). Thus, we have built four interactions. In connection with previous RPA studies [11] we have considered two interactions, labeled LM and LMtt in the following, which are zero-range interactions, based on the Landau-Migdal approach. In these interactions, the functions $v_i(r)$ of Eq. (1) are given by

$$v_i(r_{12}) \,=\, V_i\,\delta(\boldsymbol{r}_1-\boldsymbol{r}_2)\,,\quad i=1,\ldots,6\,. \tag{4}$$

In MeV fm^3 units, the values of the parameters V_i are

$$V_1 \,=\, -918\,;\; V_2 \,=\, 600\,;\; V_3 \,=\, 20\,;\; V_4 \,=\, 200\,;\; V_5 \,=\, 0\,.$$

For the LM interaction, $V_6 = 0$, while for the LMtt one, $V_6 = -150$ MeV fm^3.

Also the terms $v_i^\rho(r)$ of Eq. (1) have zero-range

$$v_i^\rho(r_{12}) \,=\, V_i^\rho\,\delta(\boldsymbol{r}_1-\boldsymbol{r}_2)\,,\quad i=1,2\,. \tag{5}$$

In MeV fm^6 units, the values of V_1^ρ are 361.0, 436.4, 492.3 and 599.0 and those of V_2^ρ are -40.0, -31.0, -150.0 and 0.0 for the ^{12}C, ^{16}O, ^{40}Ca and ^{208}Pb respectively. For ^{48}Ca, we have used the same values as for ^{40}Ca. In all the calculations within the phenomenological approach we used α=1 in Eq. (1).

These interactions have been used in RPA calculations which consider only the contribution of direct matrix elements, therefore the scalar and isospin terms of these interactions, v_1 and v_2 respectively, do not contribute to the excitation of unnatural parity states. For sake of completeness, we present here the full effective interactions, even though in this work we discuss results regarding only unnatural parity excitations.

We have also constructed two finite-range interactions with and without the tensor terms, which we labeled FRtt and FR, respectively. These two residual NN interactions are obtained from the Argonne V18 potential [24], by modifying its short range behavior to take into account short range correlations effects. In particular, the short range part of the Argonne V18 NN potential is removed and replaced by a combination of Gaussian functions. Specifically, we take

$$v_i(r) \,=\, \widetilde{V}_{18}^i(r) \,+\, \sum_{\mu=1}^{M} a_\mu^i\,\exp\left[-b_\mu^i\,(r-R_\mu^i)^2\right]\,,\quad i=1,\ldots,4\,, \tag{6}$$

where $\widetilde{V}_{18}^i(r)$ are the corresponding terms of the bare Argonne V18 potential with their short range terms set to zero. In Eq. (6) M is the number of Gaussians used in each channel. For the scalar channel we have included two Gaussians in order to obtain an attractive behavior starting from the repulsive core. The repulsive behavior is considered in the density dependent term. For the channels $i = 2$ and $i = 4$ we have used only one Gaussian. In the finite-range interactions we set to zero the spin term $i = 3$. The values of the various parameters are given in Table I. These values are common to both interactions.

In the FRtt interaction, the tensor channels are obtained by multiplying the bare V18 tensor terms by the scalar term of the two-body short range correlation function $f(r)$ of Ref. [19]

$$v_i(r) \,=\, V_{18}^i(r)\,f(r)\,,\quad i=5,6\,. \tag{7}$$

To be precise, we used the correlation functions obtained with the so-called Euler procedure and, because of the small differences between the $f(r)$ of the various nuclei [19], we have used that obtained for the ^{40}Ca in all our calculations. In the FR interaction the tensor terms are set to 0.

Finally, the density dependent terms are taken to be Gaussians:

$$v_i^\rho(r) \,=\, \alpha_i\,\exp\left(-\beta_i r^2\right)\,,\quad i=1,2\,. \tag{8}$$

In our calculations we have used $\beta_i = 1\text{fm}^{-2}$. The values of the parameter α_i are shown in Table II.

The choice of the free parameters of the finite-range interactions has been done by adopting the same criteria we used for zero-range interactions. The RPA calculations with the finite-range calculations have been done by considering

only the direct terms of the matrix elements. As in the case of the zero-range interactions we consider that the effects of the exchange terms are effectively included in the choice of the parameters values.

The self-consistent RPA calculations have been done with a Gogny interaction [16–18] which is usually expressed as

$$\begin{aligned} V_{\rm eff}(1,2) \;=\; & \sum_{i=1}^{2} \exp\left[-\frac{(\boldsymbol{r}_1-\boldsymbol{r}_2)^2}{\mu_i^2}\right] (W_i \,+\, B_i\,\hat{P}_\sigma \,-\, H_i\,\hat{P}_\tau \,-\, M_i\,\hat{P}_\sigma\,\hat{P}_\tau) \\ & + W_{LS}\;(\boldsymbol{\sigma}(1)\,+\,\boldsymbol{\sigma}(2))\;\;\overleftarrow{k}\times\delta(\boldsymbol{r}_1-\boldsymbol{r}_2)\,\vec{k} \\ & + t_0\,\left(1\,+\,x_0\,\hat{P}_\sigma\right)\,\delta(\boldsymbol{r}_1-\boldsymbol{r}_2)\,\rho^\alpha\left(\frac{1}{2}(\boldsymbol{r}_1\,+\,\boldsymbol{r}_2)\right)\,, \end{aligned} \tag{9}$$

where $\vec{k}$ is the operator of the relative momentum

$$\vec{k} \,=\, \frac{1}{2i}\;(\boldsymbol{\nabla}_1 \,-\, \boldsymbol{\nabla}_2)\;\;. \tag{10}$$

We have indicated with $\hat{P}_\sigma$ and $\hat{P}_\tau$ the usual spin and isospin exchange operators, and μ_i, W_i, B_i, H_i, M_i, W_{LS}, t_0 and x_0 are constant parameters.

The relation between the expression above of the Gogny force and that required by Eq. (1) is obtained by considering that

$$v_1(r) \;=\; W(r) \,+\, \frac{B(r)}{2} \,-\, \frac{H(r)}{2} \,-\, \frac{M(r)}{4}\,, \tag{11}$$

$$v_2(r) \;=\; \frac{B(r)}{2} \,-\, \frac{M(r)}{4}\,, \tag{12}$$

$$v_3(r) \;=\; -\frac{H(r)}{2} \,-\, \frac{M(r)}{4}\,, \tag{13}$$

$$v_4(r) \;=\; -\frac{M(r)}{4}\;. \tag{14}$$

In the equations above

$$F(r) \,=\, \sum_{i=1}^{2} F_i\,\exp\left(-\frac{r^2}{\mu_i^2}\right)\;,\quad F\equiv W,B,H,M\,. \tag{15}$$

The density dependent term of Eq. (9) can be written as:

$$t_0\,(1\,+\,x_0\,\hat{P}_\sigma)\,\rho^\alpha \,=\, \left[t_0\,\left(1\,-\,\frac{x_0}{2}\right)\,-\,\frac{t_0\,x_0}{2}\,\boldsymbol{\tau}(1)\cdot\boldsymbol{\tau}(2)\right]\,\rho^\alpha\,. \tag{16}$$

In our calculations we used the parameterization of the Gogny interaction known as D1 [16–18]. In the HF calculations we have considered all the terms of the interactions, while in the RPA calculations we have neglected the contribution of the spin-orbit term. In HF and RPA calculations both direct and exchange terms of the interaction matrix elements have been considered.

The various interactions used in our work are shown in Fig. 1 as a function of the relative momentum of the interacting pair of nucleons. In this figure, solid, dashed and dotted lines represent the D1, LMtt and FRtt interactions, respectively. Our tensor dependent interactions have been constructed by adding to the LM and FR four central channels the two tensor dependent terms. For this reason, in the figure, the LM and FR interactions are not shown, since they are identical, in the central channels, to the LMtt and FRtt interactions. The zero-range interaction terms are constant in momentum space. We point out that the spin term v_3 has been set to zero in the FR and FRtt interactions, and that LMtt does not have the pure tensor term v_5. The finite-range interactions FR, FRtt and D1 have similar asymptotic behaviour, above 4 fm^{-1}. The values of the LM and LMtt interactions fall between those of the D1, FR and FRtt interaction at $q_{12} \sim 0$.

Since we used a discrete configuration space of single particle wave functions, the solution of the RPA equations consisted in solving a homogeneous system of linear equations. For a given excitation multipole, characterized by angular momentum J and parity π, the RPA solution, obtained with standard diagonalization procedures, provides

the set of excitation energies, and, for each excited state, the full set of RPA amplitudes $X_{ph}^{J^\pi}$ and $Y_{ph}^{J^\pi}$. We could then calculate the amplitudes for the transition between ground and excited states induced by an operator $T_J(q)$ as

$$\langle J\|T_J(q)\|0\rangle \;=\; \sum_{ph} \left[X_{ph}^{J^\pi} \,\langle j_p\|T_J(q)\|j_h\rangle \;+\; (-1)^{J+j_p-j_h}\, Y_{ph}^{J^\pi} \,\langle j_h\|T_J(q)\|j_p\rangle \right] . \tag{17}$$

In the equation above $|j\rangle$ indicates the single particle wave function characterized by the set of quantum numbers including, principal quantum number, orbital angular momentum, total angular momentum j, and isospin third component. The double bars indicate the reduced matrix elements of the angular coordinates.

In this article we calculated the electromagnetic responses, which are defined as the Fourier transform of the squared moduli of the transition amplitude (17) [1]. In the plane wave Born approximation description of inelastic electron scattering experiments, these responses, which depend on the modulus of the momentum transfer q, are related to the cross section by multiplicative factors depending on kinematics variables, and to the Mott cross section [25, 26].

Since we are interested in magnetic states, the charge operator does not contribute. The operators we have used to calculate the transition amplitudes (17) are those of the convection and magnetization currents. The explicit expressions of the single particle matrix element can be found in Refs. [27, 28]. We do not consider the contribution of meson-exchange currents, which, for low-lying excited states, has been found to be negligible in comparison with the effects of the residual interaction [11, 29].

III. RESULTS OF THE PHENOMENOLOGICAL APPROACH

In this section we present our results for the low-lying magnetic states of ^{12}C, ^{16}O, ^{40}Ca, ^{48}Ca and ^{208}Pb, obtained within the phenomenological approach. For each nucleus we first present the unnatural parity low energy spectrum, we compare it with the measured spectrum, and we discuss the sensitivity of the excitation energies to the inclusion of finite-range and tensor terms contributions in the residual interaction. Then, for some specific states, we investigate the electromagnetic transverse response functions. In order to minimize the uncertainties due to the discretization of the continuum, we have selected excited states which are dominated by particle-hole (ph) pairs where the particle is in a bound state. Furthermore, we have chosen those states which exhibit the largest sensitivity to those terms of the residual interaction which are the focus of the present study. Also, we have addressed our attention to those states forming isospin doublets, because their structure (order of the states and relative splitting) is sensitive to the isospin dependent terms of the residual interactions and, more specifically, to the tensor-isospin terms we have introduced in the previous section. The interest in isospin doublets will become clearer in connection to the self-consistent calculations which will be presented in next section. In addition, we give preference to the study of those states for which experimental data are available.

A detailed discussion of the results will be done throughout this section, but we would like to anticipate that we obtained a general good description of the excitation spectra, almost independently of the effective interaction used. This indicates that we have been able to incorporate in the parameterization of the residual interaction some relevant features required by the description of the magnetic excitations. The possible discrepancies between our predictions an the experimental data have to be ascribed more to the intrinsic limitations of the RPA theory rather than to a more efficient parameterization of the interaction.

A. The ^{12}C nucleus

In Table III we compare the energies of the low-lying magnetic states of ^{12}C with the experimental values taken from Ref. [30]. In the calculation with the LM interaction we have been unable to identify the second 2^- state, since all the states higher than the first one have dominant ph components with the particle in the continuum. Apart from this case we notice that the calculated energies for each state are rather similar, independently on the interaction used. The experimental energies are reasonably well reproduced except for the 2^- states whose energies are about 4 MeV above the experimental ones.

The two most interesting cases are the 1^+ and 4^- states. For the 1^+ case we obtain two states, dominated by the $[(1p_{1/2})(1p_{3/2})^{-1}]$ proton and neutron pairs, although for the state with higher energy not negligible contributions of other ph pairs appear. The lowest energy state has isoscalar (IS) character while the state with higher energy is isovector (IV). These states correspond to the experimentally well known isospin doublet at 12.71 MeV (T=0) and 15.11 MeV (T=1) [8, 30]. The corresponding transverse response functions, or form factors, are shown as a function of the effective momentum transfer in the upper panels of Fig. 2. We use the traditional definition of the effective

momentum [1]

$$q_{\rm eff} = q\left(1 + \frac{3Z\alpha\hbar c}{2\epsilon_i R}\right), \tag{18}$$

where Z is the atomic number of the target nucleus, α is the fine structure constant, ϵ_i is the incident electron energy and R is the nuclear charge radius.

In the lower panels of the same figure, for each state considered, we show the proton (thick lines) and neutron (thin lines) contributions to the transition densities, as a function of the distance from the center of the nucleus. These transition densities have been obtained from Eq. (17) by avoiding the integration on r and eliminating the Bessel function. The behaviours of the transition densities clearly show the isospin nature of the two states. For the lower energy state, proton and neutron densities are in phase, indicating the IS nature of the excitation. The opposite happens for the second state and this is a clear signature of the IV nature of this state.

As we can see from Table III, our calculations overestimate the experimental energies of both the 1^+ states and also their splitting. The largest relative differences in the energies values are 13% and 20% for the first and second state, respectively. Despite these quantitative discrepancies with the observed energies, our calculations produce the correct sequence of isoscalar and isovector excitation with all the interactions. The inclusion of finite-range and tensor terms changes the energy values at the level of few percent. Also the response functions are not very sensitive to the use of different residual interactions as it is shown in Fig. 2. Only the responses of the IV state show some difference around the minimum at q_{eff}=1.5 fm^{-1}. The position of this minimum seems to be slightly better described by the interactions including tensor terms.

The comparison with electron scattering data [9] shows good agreement with the IS data and overestimates the experimental IV response in the region of the first maximum. A good description of the 1^+ IV transition is extremely important since this state is used in liquid scintillator neutrino detectors to identify neutral current events [31]. The figure shows that the discrepancy in the description of the IV response cannot be solved by using an overall quenching factor. While the first peak is overestimated by almost a factor two, the second peak is rather well reproduced. The difficulty in describing the IV 1^+ state is a common characteristic of the RPA calculations [32–36], and produces an overestimation of the experimental total neutrino ^{12}C cross sections measured in the LNSD [31, 37, 38] and KARMEN [39] experiments. In order to solve the problem, the presence of strong pairing effects has been advocated [40], with the idea that the shell closure in the ^{12}C nucleus is not a good approximation. We have to remark, however, that the problem of describing the the IV 1^+ state is present also in other doubly magic nuclei where pairing correlations are negligible [23]. The size of the first maximum of the 1^+ IV response in ^{12}C is well reproduced by microscopic *ab initio* shell model calculations [41], but the shape is completely wrong. These calculations produce the first minimum of the response at 2 fm^{-1}, and they are completely missing both size and shape of the second maximum.

We consider now the 4^- states which also form an isospin doublet. These states are dominated by the linear combination of the stretched $[(1d_{5/2})(1p_{3/2})^{-1}]$ excitations. In our calculations the $1d_{5/2}$ state is bound in the neutron case with an energy of -1.1 MeV, and it shows a sharp resonance at 2.0 MeV in the case of protons. The MF excitation energies are the single particle energy differences, which for this ph transitions are 17.96 and 17.62 MeV for protons and neutrons, respectively. The RPA calculations mix the proton and neutron ph transitions and in our calculations, independently of the interaction used, the isoscalar state has lower energy than the isovector one. The results shown in Table III indicate that the residual interaction produces solutions with energies higher than those given by the MF solution. In this situation the role of the finite-range of the force is not negligible. The upward shift of the RPA solutions is reduced by only 0.5 of MeV for the IS state, but by 1.7 MeV for the IV state. The experimental IS energy is better reproduced by the zero-range interaction, while the IV energy is much better described by the FRtt interaction.

We show in Fig. 3, the electromagnetic responses for the two 4^- states. We compare the IV responses to the available experimental data [4]. The IS responses show some sensitivity to the use of the residual interaction. The inclusion of the tensor terms and of the finite-range, reduces the size of the response. The results of the IV responses are rather independent of the residual interaction and the experimental data are rather well reproduced.

Finally we observe that our model also produces 2^- states, however, as said before, their energies are in large disagreement with data. The same occurs when the corresponding responses are compared. This might be due to the presence, in these states, of sizable contributions from ph pairs having a particle in the continuum, which bring in further uncertainties, as our procedure discretizes the continuum.

B. The ^{16}O nucleus

The spectrum of the low-lying magnetic states obtained with the four interactions is presented in Table IV, where it is compared with the experimental spectrum [30]. All the states have negative parity and, since the p-shell is closed

for both protons and neutrons, this indicates that they are dominated by ph transitions involving confining shells. The order of the various states is reproduced by our calculations. The magnetic state with lowest energy is a 2^- state, as in the experimental spectrum. Our energy eigenvalues are however overestimating the experimental value of about 30%, independently of the interaction used. This finding is contrary to our expectations, since this state is dominated by the $[(1d_{5/2})(1p_{1/2})^{-1}]$ bound proton and neutron transitions, therefore it should be well described by our approach. Also for the transition density we have found [22] a remarkable disagreement with the experimental data [9]. These facts indicate the presence in this 2^- state of effects beyond the description capability of the RPA.

The following states in our spectrum are two 0^- states which can be identified in the experimental spectrum [30]. These states are dominated by the $[(2s_{1/2})(1p_{1/2})^{-1}]$ proton and neutron transitions. The effect of the tensor term of the interaction on the energy values is not negligible. Since these states are not excited by electromagnetic probes, at least in the one-photon exchange picture, we have calculated neutrino and antineutrino cross sections [22] and we have found large sensitivity to the tensor force. This point deserves a more detailed investigation, for example by calculating the excitations induced by hadronic probes.

The 4^- states, dominated by $[(1d_{5/2})(1p_{3/2})^{-1}]$ protons and neutrons ph excitations, form an isospin doublet. Also in this case the energy of the IS state is lower than that of the IV one, correctly describing the experimental findings. The IS energy eigenvalues are rather insensitive to the presence of tensor terms; they are however rather sensitive to the use of finite-range interactions. In the IV case, both tensor terms and finite-range affect the energy value. The electromagnetic responses for both states are shown in Fig. 4 and compared with the experimental data of Ref. [9]. In both cases the position of the maximum of our calculations is slightly lower than the experimental one. The IS state shows some sensitivity to the residual interaction. The inclusion of the tensor term and of the finite-range contributes to lower the response and this slightly improves the agreement with the data. The IV response is less sensitive to the changes of the interaction. We obtain a general good agreement with the data.

C. The ^{40}Ca nucleus

The spectrum of the magnetic states of the ^{40}Ca nucleus is given in Table V. The global closure of the *s*-*d* shell, for both protons and neutrons, implies that the low-energy spectrum is composed only by negative parity states. Our RPA calculations reproduce the correct sequence of the states, independently of the interaction used. The energy eigenvalues do not show large sensitivity to the choice of the interaction. We overestimate the energy of the first 4^- state, while the energies of the other states are better reproduced.

The response functions of the 2^- and 4^- states are shown in Fig. 5 and compared with the available experimental data [42]. The response of the lowest 2^- state is almost insensitive to the choice of the residual interaction. The electromagnetic response of the other 2^- state shows larger sensitivity to the interaction used in the RPA calculation. The shapes of the responses are remarkably modified by the finite-range and by the tensor terms. The tensor term reduces the response in the first maximum and compresses the second bump of the response. The data are not accurate enough to select among the various results.

The response of the lowest 4^- state indicates that the presence of the finite-range increases the peak value, while the tensor term reduces it. The same effect is present also in the response of the other 4^- state, even if with smaller size. In this latter case we have the possibility of making comparison with experimental data [42]. There is no similarity in size and shape between our results and the data.

D. The ^{48}Ca nucleus

In Table VI we present the low-energy magnetic spectrum of ^{48}Ca. In these calculations we have adopted the residual interactions used for the ^{40}Ca calculations. The ^{48}Ca spectrum contains both negative and positive parity states, the latter dominated by single particle excitations of the $1f_{7/2}$ neutron hole. Globally, we obtain a reasonable agreement between the measured and calculated energies, however, the correct sequence of the excited states is not exactly reproduced. In each calculation we obtain a 6^- state with energies larger than those of the 1^+ state, while experimentally the opposite occurs. This disagreement is due to the overestimation of the 6^- state energy by about 2.5 MeV. The energy eigenvalues presented in Table VI do not show remarkable sensitivity to the different interactions used in the RPA calculations.

More interesting is the study of the electromagnetic responses of these states, shown in Fig. 6 and compared to the available experimental data [6, 43]. Noticeable sensitivity to the choice of the residual interaction is shown only for the 2^-, 6^-, and, with smaller effects, 4^- and 1^+ states. As already mentioned, the positive parity states are dominated by the excitation of the $1f_{7/2}$ neutron hole, therefore the residual interaction plays a minor role and the results are rather similar to those of the MF. Effects of the use of different interactions are present in the 1^+ response

only at the third maximum and at the first two maxima of the 3^+ state. The experimental data of the 3^+ and 5^+ are rather well reproduced. The same does not occur with the 1^+ state where other mechanisms beyond RPA (second order core polarization, tensor correlations and Δ excitations) must be taken into account to reach a good agreement between theory and experiment [44].

The situation for the negative parity states is more complicated. There is no common trend related to the inclusion of the various ingredients of the interactions. For example, the tensor term increases the responses of the 4^- and 6^- states, while it lowers that of the 2^- state. The 2^- and 4^- experimental responses are rather well reproduced. Similar results have been obtained in Ref. [45] where the Jülich-Stony Brook interaction [46] with the tensor terms reduced by ∼30-60% has been used. We have encountered problems in the description of the 6^- response. On the other hand, we have already pointed out the difficulties found in describing the excitation energy of this state.

E. The ^{208}Pb nucleus

The energies of the low-lying magnetic states of ^{208}Pb are presented in Table VII and compared with the experimental ones. The sequence of the states is quite well reproduced. The are some exceptions, but these occur in situations where the energy differences are of the order of few tens of keV, an energy resolution smaller than the accuracy we attribute to our results. The global picture emerging from the observation of Table VII is that the various interactions produce small differences in the energy eigenvalues.

The investigation of the electromagnetic responses provides more information. We start our discussion with the 12^- responses which have been quite often studied in the past [11, 47, 48] because of their, apparently, simple ph structure. They are, in fact, mainly composed by two ph pairs, the proton $[(1i_{13/2})(1h_{11/2})^{-1}]$ and neutron $[(1j_{15/2})(1i_{13/2})^{-1}]$ transitions. The lower 12^- state, experimentally found at 6.43 MeV, is neutron dominated, while the state at higher energy, 7.08 MeV, is dominated by the proton transition. Our calculations produce the correct order of these two states, and the RPA energies agree well with the experimental values, especially the lower one. We must recall, however, that this state has been used to set the values of the interaction parameters. The calculated energies of the higher state overestimate the experimental value, but the discrepancies are below 10%. The electromagnetic responses are shown in the right panels of Fig. 7 and are compared with the data of Ref. [3]. The responses relative to the higher state, lower panel, show a reasonable agreement with the data and it is almost insensitive to the choice of the residual interaction. On the contrary, the responses of the neutronic state, upper panel, are extremely sensitive to the inclusion in the interaction of both finite-range and tensor terms. These effects improve the agreement with the data, but the calculated curves still underestimate the measured response. The disagreement could be reduced by increasing the magnitude of the tensor part of the interaction. We found, however, that this produces a general worsening of the magnetic spectrum of ^{208}Pb, and also of the other nuclei we have considered. One of the features obtained by this procedure is the inversion of the IS and IV 1^+ states.

In the left panels of Fig. 7 we present the responses of the 10^- states which show some sensitivity to the inclusion of the tensor contribution in the residual interaction. All interactions can reproduce the magnitude of the responses, but only the inclusion of the tensor terms allows a good description of the second peak in both 10^- states. Improvements in the precision of experimental data around $q = 2.5$ fm^{-1} would be particularly important to study the tensor component of the residual interaction.

The energies of the 1^+ states are rather well reproduced with all the residual interactions, for the isoscalar state at 5.85 MeV and for the isovector state at 7.30 MeV. We should point out that the IV state is so fragmented that this energy value is an estimate based on an accurate analysis of the photon scattering data [23]. The electromagnetic responses are plotted in Fig. 8, and for the IS state (upper panel) we compare them with the data [5]. For this state, all the curves reproduce the q-dependence of the data but not for low q values, where the theoretical responses are well below the data. Unfortunately there are no data in the region $q < 0.5$ fm^{-1} where the various responses differ more. In the IV case (lower panel) the differences between the various results appear at large q values. This is, however, a theoretical speculation, since, as we have already said, experimentally the IV state is extremely fragmented, and cannot be described within the RPA theory.

The 9^+, 11^+ and 14^- states are dominated by a single particle-hole excitation, with the exception of the lower energy 9^+ state, where a small contribution of the proton $[(2f_{7/2})(1h_{11/2})^{-1}]$ transition is present besides the dominant neutron $[(2g_{9/2})(1i_{13/2})^{-1}]$ one. For this state, the calculated transverse responses, presented in the upper left panel of Fig. 9, show three peaks, and this behavior is compatible with the data. On the other hand, the position of the experimental points of the other 9^+ state, shown in the lower left panel of the same figure, is very different from the shape of the theoretical responses, which show some dependence on the residual interaction. Analogous problems are found also for the 11^+ states, whose responses are plotted in the right panels of Fig. 9.

To complete our survey we show in Fig. 10 the electromagnetic response of the 14^- state. Its nature of almost pure ph transition is evident since there is no dependence on the residual interaction, as pointed out in the literature

(see for example [49]).

IV. RESULTS OF SELF-CONSISTENT CALCULATIONS

In the previous section we have presented the results of the phenomenological approach. We would like to point out that the study of the full set of magnetic states, together with their electromagnetic responses, can be used to test the validity of the effective interactions used in RPA calculations. In order to give an example of this potentiality, we present here some selected results we have obtained with the Gogny D1 interaction [16–18].

In the RPA calculations we have neglected the contribution of the spin-orbit term of the interaction. This is a good approximation if also the contribution of the residual Coulomb interaction is neglected [50], as we do in our calculations. In the phenomenological approach we have calculated only the direct matrix elements of the interaction, arguing that our parameterization procedure effectively takes care of the exchange diagrams contributions. By using the D1 interaction we have considered both direct and exchange matrix elements, since the interaction has been constructed to reproduce ground state properties within the Hartree-Fock approach, therefore it has not been tailored for RPA calculations. In the phenomenological approach the link between the properties of the excitation spectrum and the various parts of the interaction is straightforward, while in the case of the D1 interaction the situation is more complicated since each interaction term contributes to the other channels through the exchange diagrams. For example, in the phenomenological approach, scalar and isospin channels do not contribute to the excitation of unnatural parity states. This is not longer true in the case of the calculations with the D1 interaction, since these two channels produce a contribution in the spin and spin-isospin channels in the exchange diagrams. To complete the information about our RPA calculations we point out that we have considered the so-called rearrangement terms related to the density dependent terms of the interaction. These terms arise by considering the effective interaction as the second derivative of the energy with respect to the single particle density [51]. Quantitatively, the contributions of these terms are negligible in all the cases we have considered.

In the following, we present the results of two types of calculations done with the D1 interaction. The first one has been done with the single particle wave functions and energies used in the phenomenological approach. The results of these calculations will be presented in Figs. 11, 12 and 13 by the dotted lines. The second type of calculations is fully self-consistent, i.e. the single particle basis is produced by a Hartree-Fock calculation done with the same interaction used in RPA. The results of these calculations are shown in the figures mentioned above as dashed lines. The comparison between these results enables us to distinguish between the role played by the single particle basis and that played by the residual interaction. In the figures, the full lines show the results obtained in the phenomenological approach by using the FR interaction. This interaction has finite-range but does not include the tensor terms, therefore, among the four interactions we have defined, it is the most similar to the D1 interaction.

We start our discussion with the 1^+ isospin doublet in ^{12}C whose electromagnetic responses are shown in Fig. 11. The striking result is that when the D1 interaction is used the position of the IS and IV states is inverted. The D1 responses plotted in the upper panel of the figure are those obtained with the RPA amplitudes of the higher energy 1^+ state. On the other hand, the D1 responses in the lower panel are those obtained for the lower energy 1^+ state. The role of the single particle basis is particularly evident in the IS state where the result obtained with the D1 interaction and the single particle wave functions and energies used in phenomenological approach (dotted curve) is completely different from that of the self-consistent calculation (dashed curve). In the case of the IV state this effect is less evident.

We found the inversion of the IS and IV partner states in all the cases we have investigated, as it is shown as example in Fig. 12 for a set of 4^- states and in Fig. 13 for the 1^+ states in ^{208}Pb . It is important to realize that the inversion is obtained in both the RPA calculations done with the D1 interaction and therefore it does not depend on the single particle basis, but it is related to the characteristics of the interaction. We have repeated our calculations with another Gogny-like force with different values of the parameters, the D1S interaction [52]. Also in this case we observed the inversion of the isospin partner states.

V. CONCLUSIONS

We have studied the magnetic excitation spectrum of doubly closed nuclei to investigate the properties of the spin, spin-isospin and tensor terms of the effective interaction. In a phenomenological approach, where the single particle basis is obtained by using Woods-Saxon wells, we have constructed four interactions which have enabled us to reproduce with the same degree of accuracy the energy of specific magnetic excited states in ^{12}C , ^{16}O , ^{40}Ca , ^{48}Ca and ^{208}Pb . We have built first a zero-range interaction having only the four central channels, and we have progressively complicated the structure of the interaction by adding tensor terms and finite-range. Our RPA calculations done

for a large number of magnetic excitations indicate that the four interactions are able to describe with reasonable accuracy the experimental spectra and the electromagnetic responses. We have found few cases where the role of the finite-range and of the tensor terms is relevant, for example the neutronic 12^- state of ^{208}Pb shown in Fig. 7. In general our phenomenological calculations have been able to describe the shapes and magnitudes of the experimental responses. However, also for the responses we have found some cases of large disagreement, as for example the 4^- state of ^{40}Ca at 7.66 MeV, shown in Fig. 5. These cases are more related to the inadequacy of the RPA description rather than to a bad parameterization of the interaction.

The validity of our approach has been tested on the Gogny D1 interaction. We have repeated the calculations of the magnetic excitation of all the states considered in the phenomenological approach by using this interaction. The calculations have been done with the single particle basis used in the phenomenological approach and also in a fully self-consistent approach, where the single particle basis has been generated by a Hartree-Fock calculation. The striking result we have obtained is that the D1 interaction inverts the energy sequence of isospin partner excitations, independently of the single particle basis adopted and for all the nuclei studied. For a fixed multipolarity the experimental evidence is that the IS excitation has lower energy than the IV one, while this order is inverted in the RPA calculations with the D1 interaction. In these circumstances, the role of both the spin-orbit and the residual Coulomb terms of the interaction, which are neglected in our RPA calculations, should be investigated in order to control the validity of the D1-like interactions for this kind of calculations.

Improvements of Gogny type of interaction have recently attracted a lot of attention [53–55], since self-consistent calculations have a wider predictive power than phenomenological approaches. The description of exotic nuclei, which will be produced and studied in the future nuclear physics facilities, requires the use of well grounded self-consistent calculations. We think that the analysis of the magnetic spectra and of their electromagnetic properties is an important filter to select the nucleon-nucleon interactions to be used in the effective nuclear theories.

Acknowledgments

This work has been partially supported by the Spanish Ministerio de Ciencia e Innovación under contract FPA2008-04688 and by the Junta de Andalucía (FQM0220).

[1] J. Heisenberg and H. P. Blok, Ann. Rev. Nucl. Part. Sci. **33**, 569 (1983).
[2] T. W. Donnelly, J. D. Walecka, I. Sick, and E. B. Hughes, Phys. Rev. Lett. **21**, 1196 (1968).
[3] J. Lichtenstadt and et al., Phys. Rev. C **20**, 497 (1979).
[4] R. S. Hicks and et al., Phys. Rev. C **30**, 1 (1984).
[5] S. Müller and et al., Phys. Rev. Lett. **54**, 293 (1985).
[6] J. E. Wise and et al., Phys. Rev. C **31**, 1699 (1985).
[7] T. N. Buti and et al., Phys. Rev. C **33**, 755 (1986).
[8] R. S. Hicks and et al., Phys. Rev. C **36**, 485 (1987).
[9] C. E. Hyde-Wright et al., Phys. Rev. C **35**, 880 (1987).
[10] J. Connelly and et al., Phys. Rev. C **45**, 2711 (1992).
[11] G. Co' and A. M. Lallena, Nucl. Phys. A **510**, 139 (1990).
[12] A. M. Lallena, Phys. Rev. C **48**, 344 (1993).
[13] A. M. Lallena, Nucl. Phys. A **615**, 325 (1996).
[14] A. Migdal, *Theory of finite Fermi systems and applications to atomic nuclei* (Interscience, London, 1967).
[15] J. Speth, E. Werner, and W. Wild, Phys. Rep. **33**, 127 (1977).
[16] D. Gogny, *Nuclear selfconsistent fields* (G.Ripka and M.Porneuf, North Holland, 1975).
[17] J. P. Blaizot and D. Gogny, Nucl. Phys. A **284**, 429 (1977).
[18] J. Dechargè and D. Gogny, Phys. Rev. C **21**, 1568 (1980).
[19] F. Arias de Saavedra, C. Bisconti, G. Co', and A. Fabrocini, Phys. Rep. **450**, 1 (2007).
[20] G. Co' and A. M. Lallena, Nuov. Cim. A **111**, 527 (1998).
[21] A. R. Bautista, G. Co', and A. M. Lallena, Nuov. Cim. A **112**, 1117 (1999).
[22] V. De Donno, Ph.D. thesis, Università di Lecce (Italy) (2008), unpublished.
[23] R. M. Laszewski and J. Wambach, Comments Nucl. Part. Phys. **14**, 321 (1985).
[24] R. B. Wiringa, V. G. J. Stoks, and R. Schiavilla, Phys. Rev. C **51**, 38 (1995).
[25] T. de Forest Jr. and J. Walecka, Adv. Phys. NY **45**, 365 (1966).
[26] S. Boffi, C. Giusti, F. Pacati, and M. Radici, *Electromagnetic response of atomic nuclei* (Clarendon, Oxford, 1996).
[27] G. Co' and S. Krewald, Nucl. Phys. A **433**, 392 (1985).
[28] J. E. Amaro, G. Co', and A. M. Lallena, Ann. Phys. (N.Y.) **221**, 306 (1993).
[29] J. S. Dehesa, S. Krewald, A. M. Lallena, and T. Donnelly, Nucl. Phys. A **436**, 573 (1985).

[30] C. M. Lederer and V. S. Shirley, *Table of isotopes, 7th ed.* (John Wiley and sons, New York, 1978).
[31] N. Y. Agafonova and et al., Astrop. Phys. **27**, 254 (2007).
[32] E. Kolbe, K. Langanke, and S. Krewald, Phys. Rev. C **49**, 1122 (1994).
[33] E. Kolbe, K. Langanke, F. K. Thielemann, and P. Vogel, Phys. Rev. C **52**, 3437 (1995).
[34] C. Volpe, N. Auerbach, G. Colò, T. Suzuki, and N. VanGiai, Phys. Rev. C **62**, 015501 (2000).
[35] G. Co', Acta Phys. Pol. B **37**, 2235 (2006).
[36] G. Co', V. De Donno, and C. Maieron (2009), contribution to NOW08, arXiv:0812.2765 (nucl-th).
[37] C. Athanassopoulos and et al., Phys. Rev. C **58**, 2489 (1998).
[38] A. Aguilar and et al., Phys. Rev. D **64**, 112007 (2001).
[39] K. Eitel and et al., Nucl. Phys. B (Proc. Suppl.) **77**, 212 (1999).
[40] F. Krmpotić, A. Samana, and A. Mariano, Phys. Rev. C **71**, 044319 (2005).
[41] A. C. Hayes, P. Navrátil, and J. P. Vary, Phys. Rev. Lett. **91**, 012502 (2003).
[42] C. F. Williamson and et al. (1987), abst. subm. to PANIC (JAPAN), unpublished.
[43] W. Steffen and et al., Nucl. Phys. A **404**, 413 (1983).
[44] J. E. Amaro and A. M. Lallena, Phys. Lett. B **261**, 229 (1991).
[45] J. E. Amaro and A. M. Lallena, Mod. Phys. Lett. A **7**, 3029 (1992).
[46] J. Speth, V. Klemt, J. Wambach, and G. E. Brown, Nucl. Phys. A **343**, 382 (1980).
[47] S. Krewald and J. Speth, Phys. Rev. Lett. **45**, 417 (1980).
[48] A. M. Lallena, Nucl. Phys. A **489**, 70 (1988).
[49] N. M. Hintz, A. M. Lallena, and A. Sethi, Phys. Rev. C **45**, 1098 (1992).
[50] T. Sil, S. Shlomo, B. K. Agrawal, and P. G. Reinhard, Phys. Rev. C **73**, 034316 (2006).
[51] P. Ring and P. Schuck, *The nuclear many-body problem* (Springer, Berlin, 1980).
[52] J. F. Berger, M. Girod, and D. Gogny, Comp. Phys. Commun. **63**, 365 (1991).
[53] T. Otsuka, T. Matsuo, and D. Abe, Phys. Rev. Lett. **97**, 162501 (2006).
[54] F. Chappert and M. Girod, Int. J. Mod. Phys. E **15**, 339 (2006).
[55] T. Otsuka and D. Abe, Prog. Part. Nucl. Phys. **59**, 425 (2007).

channel	a_1^i [MeV]	b_1^i [fm^{-2}]	R_1^i [fm]	a_2^i [MeV]	b_2^i [fm^{-2}]	R_2^i [fm]
$i=1$	600.0	4.0	0.5	-200.0	20.0	0.0
$i=2$	300.0	7.0	0.5			
$i=4$	-40.0	4.5	0.5			

Table I: Parameters of the Gaussian functions of the FR and FRtt interactions (see Eq. (6)). The spin terms, $i=3$, have been set to zero.

	FR		FRtt	
	α_1	α_2	α_1	α_2
nucleus	[MeV]	[MeV]	[MeV]	[MeV]
^{12}C	133.8	-120.0	133.8	-125.0
^{16}O	163.4	-95.0	163.6	-95.0
^{40}Ca	194.7	-50.0	194.6	-50.0
^{208}Pb	240.0	-25.0	240.0	-25.0

Table II: Parameters of the density dependent terms of the FR and FRtt interactions (see Eq. (8)).

^{12}C					
J^π	LM	LMtt	FR	FRtt	exp
2^-	16.26	16.20	16.07	16.03	11.83
1^+	14.41	14.41	13.89	13.87	12.71
2^-	—	17.26	17.23	17.14	13.35
1^+	18.13	17.97	18.17	18.05	15.11
4^-	18.21	18.21	17.78	17.75	18.27
4^-	21.70	20.80	19.92	19.49	19.50

Table III: Low-lying spectrum of the unnatural parity, magnetic, states in ^{12}C. The energies are expressed in MeV. The experimental values are from Ref. [30].

^{16}O					
J^π	LM	LMtt	FR	FRtt	exp
2^-	11.80	11.80	11.51	11.51	8.87
0^-	12.33	11.19	12.15	11.84	10.96
0^-	—	12.39	13.13	12.23	12.80
4^-	18.15	18.15	17.75	17.73	17.79
4^-	21.41	20.59	19.88	19.45	18.98

Table IV: Same as in Table III but for ^{16}O.

^{40}Ca					
J^π	LM	LMtt	FR	FRtt	exp
4^-	6.86	6.88	6.78	6.80	5.61
2^-	7.21	7.20	6.91	6.90	7.53
4^-	7.52	7.59	7.42	7.47	7.66
2^-	8.90	8.44	8.76	8.58	8.42

Table V: Same as in Table III but for ^{40}Ca.

^{48}Ca					
J^π	LM	LMtt	FR	FRtt	exp
3^+	5.03	4.99	4.96	4.94	4.61
5^+	5.26	5.16	5.04	4.98	5.15
4^-	6.44	6.41	6.36	6.35	6.10
2^-	7.53	7.06	7.30	7.10	6.89
6^-	11.29	11.31	11.01	10.99	8.56
1^+	9.65	9.38	9.68	9.50	10.23

Table VI: Same as in Table III but for ^{48}Ca.

^{208}Pb					
J^π	LM	LMtt	FR	FRtt	exp
4^-	3.52	3.50	3.50	3.49	3.48
6^-	4.04	4.04	4.03	4.03	3.92
2^-	4.30	4.21	4.23	4.20	4.23
9^+	5.14	5.11	5.11	5.09	5.01
9^+	5.45	5.45	5.44	5.44	5.26
0^-	5.64	5.38	5.54	5.42	5.28
11^+	5.25	5.20	5.14	5.12	5.29
1^+	5.92	5.89	5.72	5.70	5.85
11^+	5.88	5.89	5.86	5.87	5.86
10^-	6.64	6.56	6.57	6.53	6.28
12^-	6.66	6.61	6.57	6.54	6.43
14^-	6.99	6.84	6.66	6.59	6.74
10^-	7.44	7.22	7.32	7.23	6.88
12^-	7.72	7.55	7.41	7.32	7.08
1^+	7.38	6.77	7.64	7.48	7.30

Table VII: Same as in Table III but for ^{208}Pb.

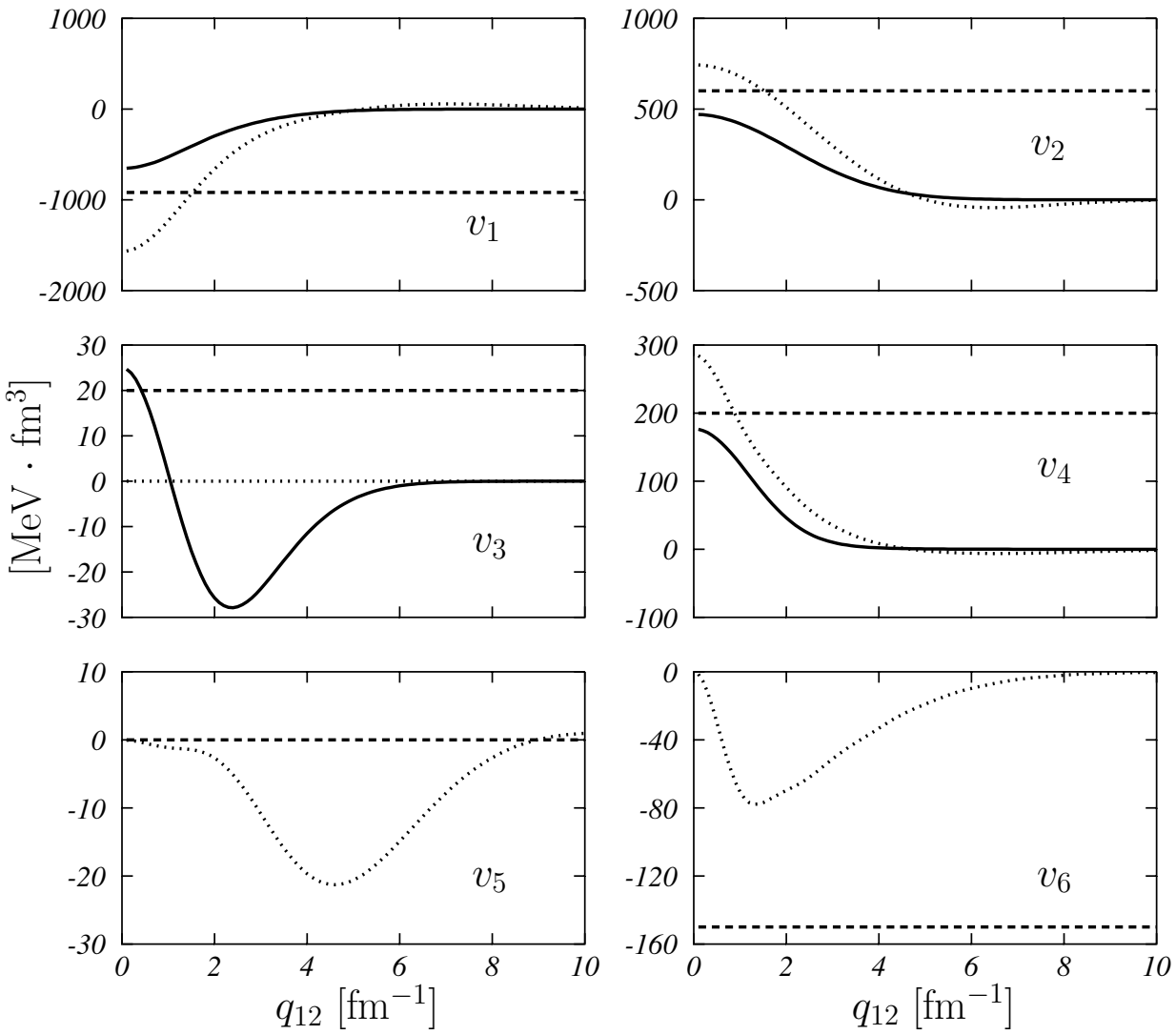

Figure 1: The effective NN interactions used in this work as a function of the relative momentum. The solid lines represent the D1, the dashed lines the LMtt and dotted lines the FRtt interactions respectively. The central channels $v_1 ... v_4$ of LMtt and FRtt interactions are identical to those of the LM and FR interactions respectively.

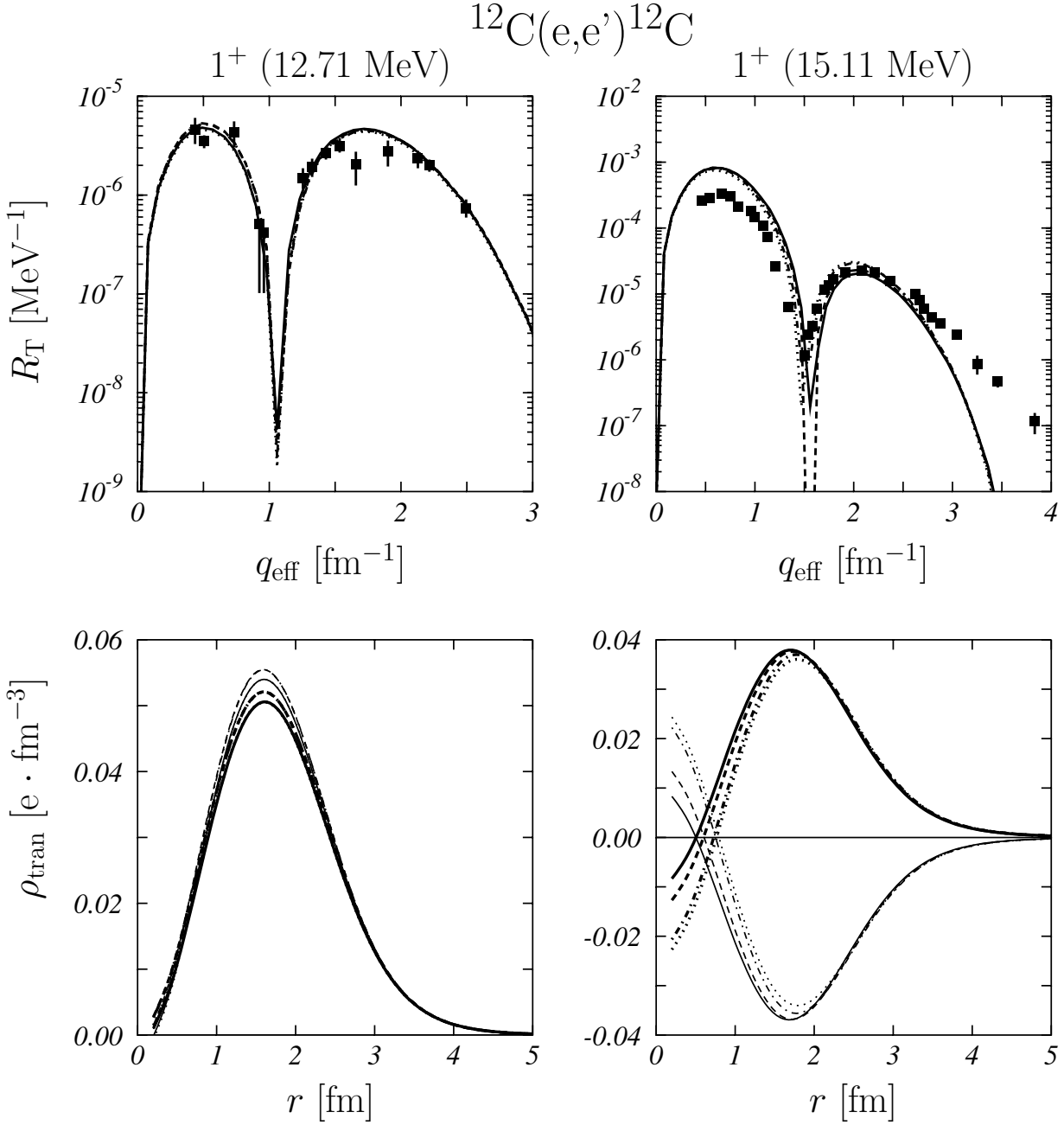

Figure 2: The Upper panels show the electromagnetic responses of the 1^+ states in ^{12}C . The data are taken from [9]. The various lines indicate the interaction used in the RPA calculation, specifically, LM (solid), LMtt (dotted), FR (dashed) and FRtt (dashed-dotted). The lower panels show protons (thick lines) and neutrons (thin lines) contributions to the transition densities of the two states. The line types have the same meaning as in the upper panels.

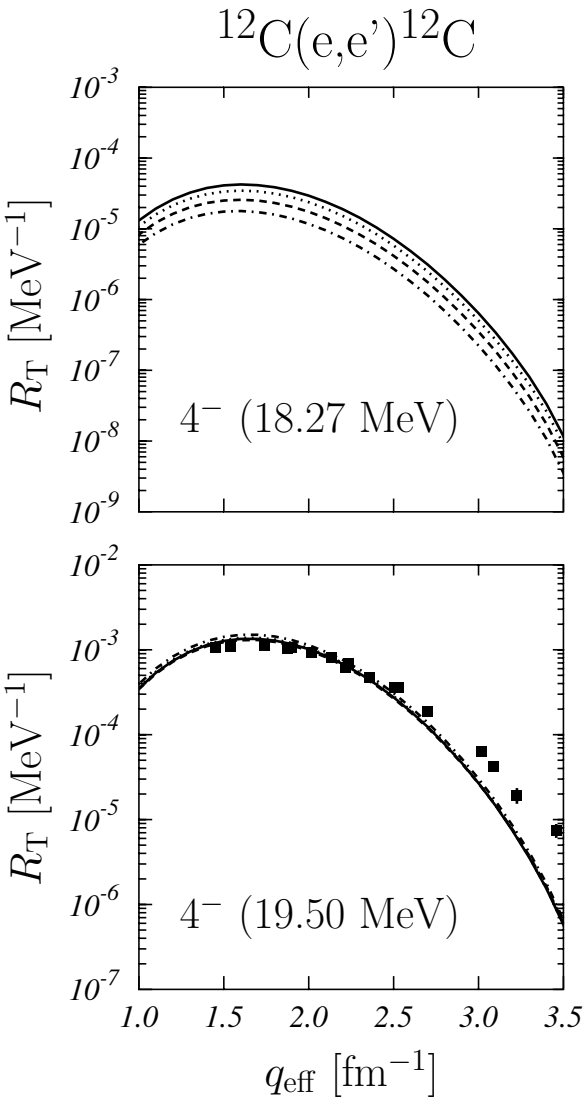

Figure 3: Electromagnetic responses of the 4^- states in ^{12}C . The meaning of the lines is the same as in Fig. 2. The data are taken from [4].

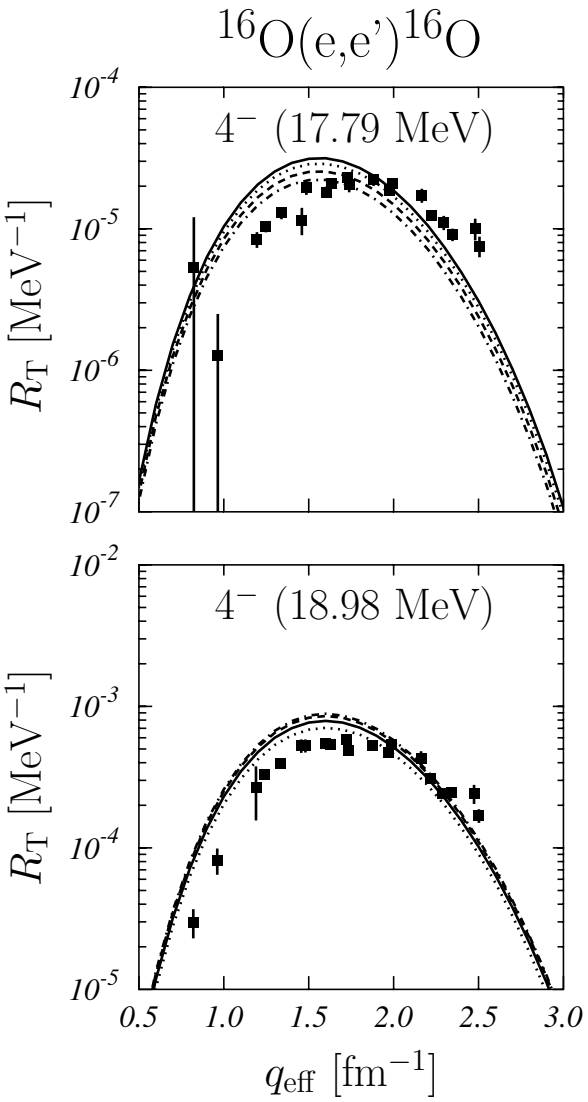

Figure 4: Electromagnetic responses of the 4^- states in ^{16}O. The meaning of the lines is the same as in Fig. 2. The data are taken from [9].

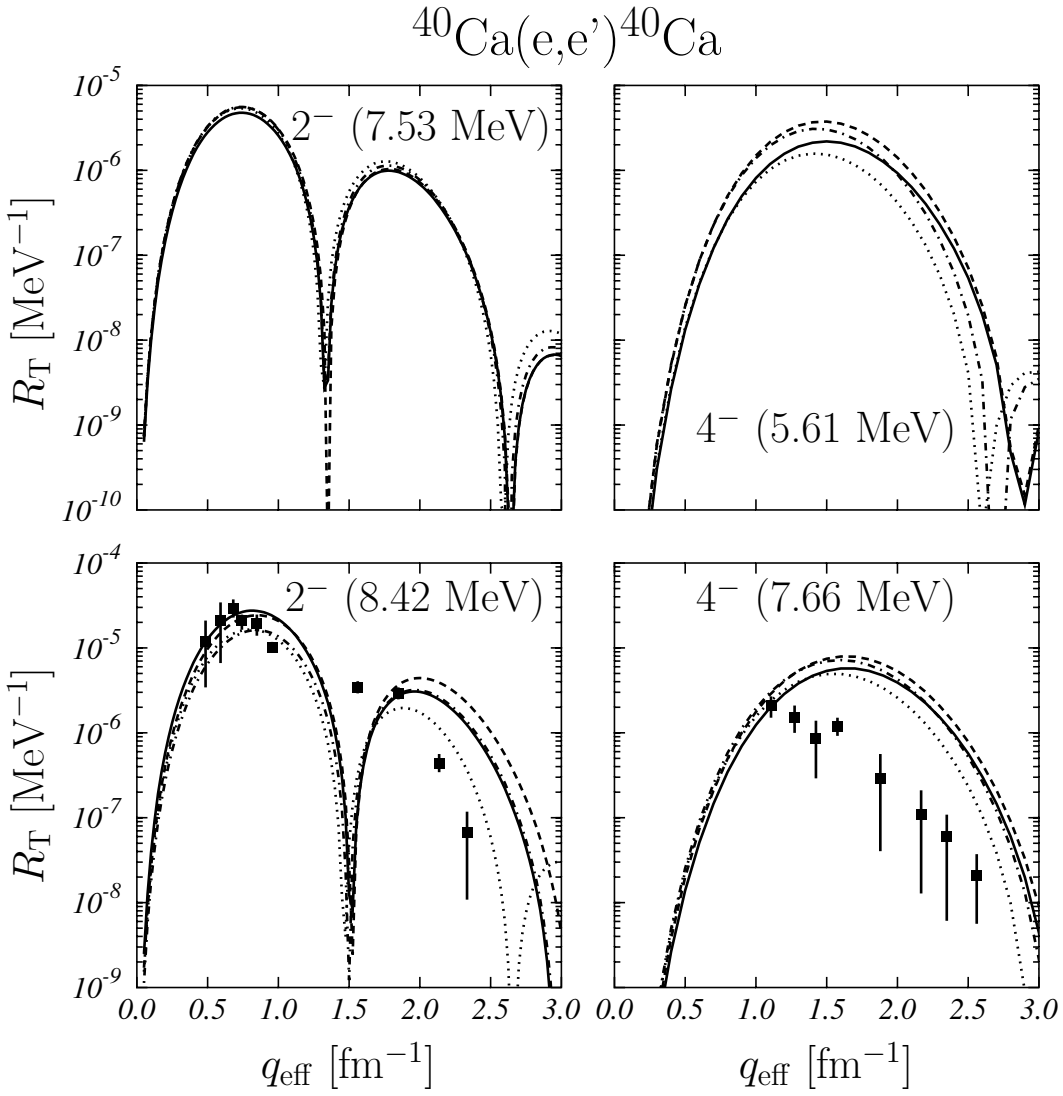

Figure 5: Electromagnetic responses of the 2^- and 4^- states in ^{40}Ca. The meaning of the lines is the same as in Fig. 2. The data are taken from [42].

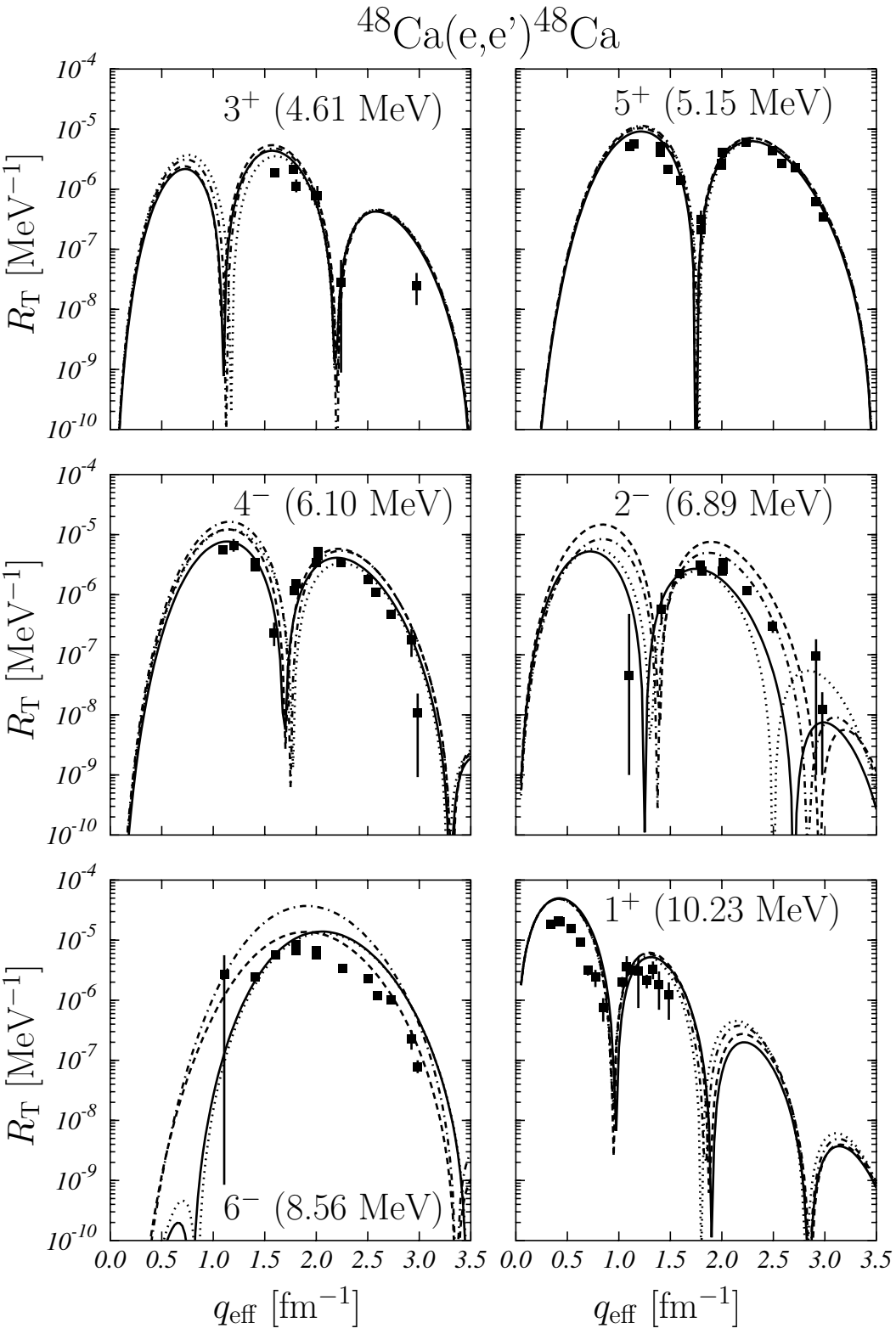

Figure 6: Electromagnetic responses of magnetic states in ^{48}Ca. The meaning of the lines is the same as in Fig. 2. The data are taken from [6, 43].

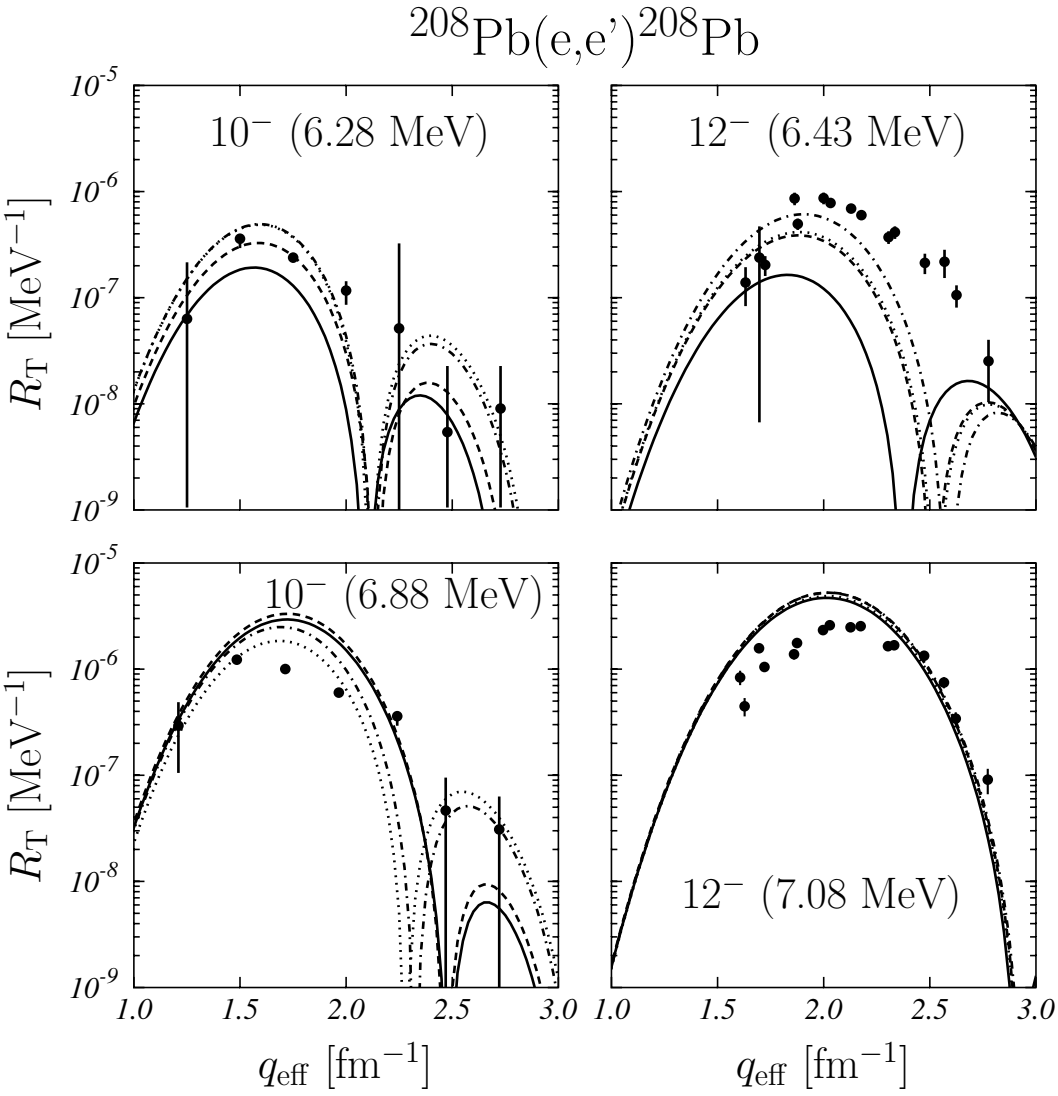

Figure 7: Electromagnetic responses of the 10^- and 12^- states in ^{208}Pb. The meaning of the lines is the same as in Fig. 2. The data are taken from [3].

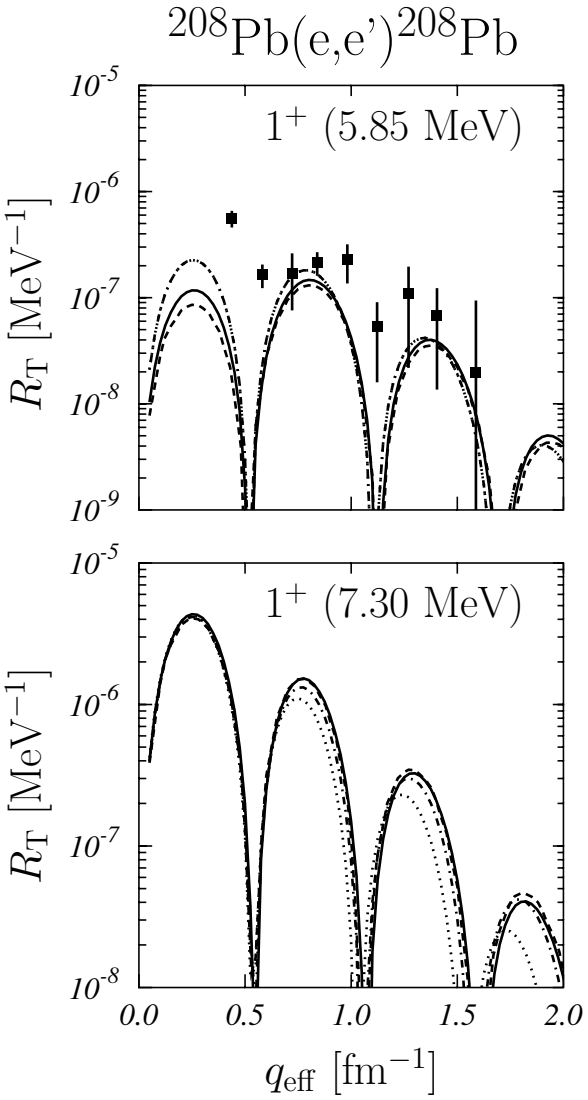

Figure 8: Electromagnetic responses of the 1^+ states in ^{208}Pb. The meaning of the lines is the same as in Fig. 2. The data are taken from [5].

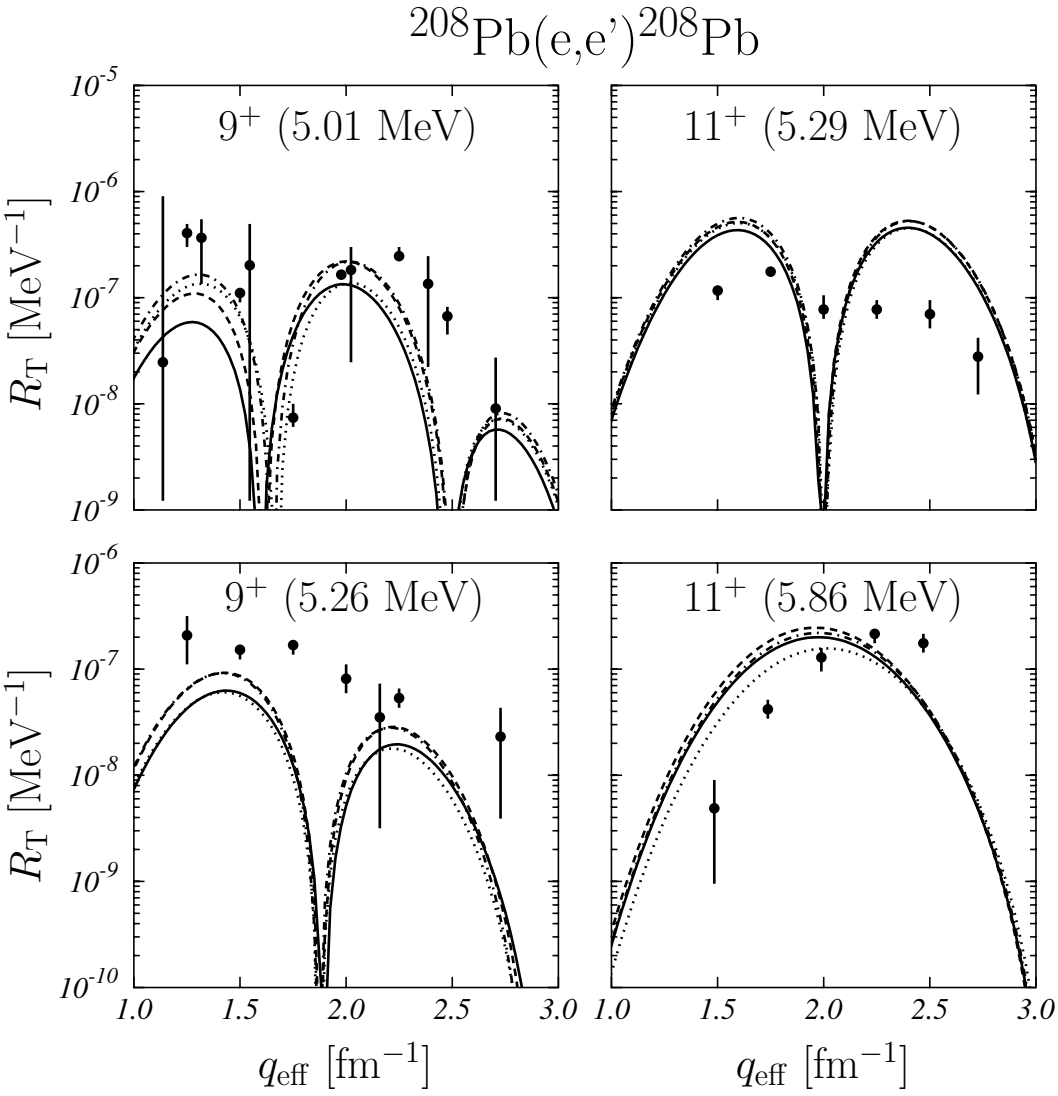

Figure 9: Electromagnetic responses of the 9^+ and 11^+ states in ^{208}Pb. The meaning of the lines is the same as in Fig. 2. The data are taken from [3].

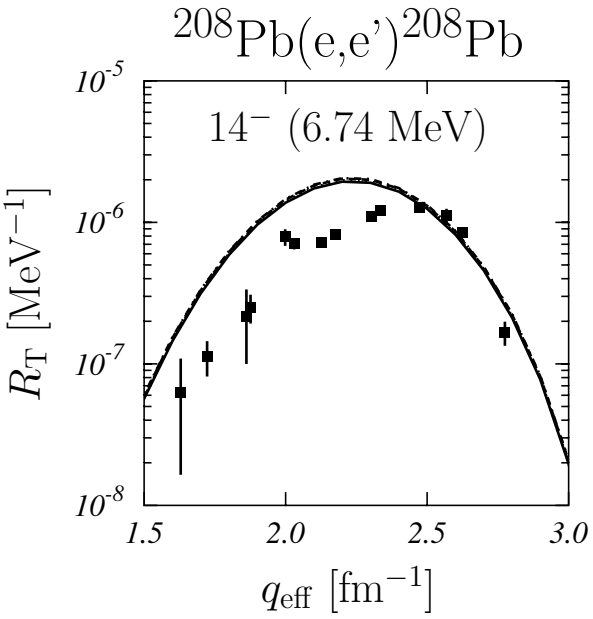

Figure 10: Electromagnetic responses of the 14^- states in ^{208}Pb. The meaning of the lines is the same as in Fig. 2. The data are taken from [3].

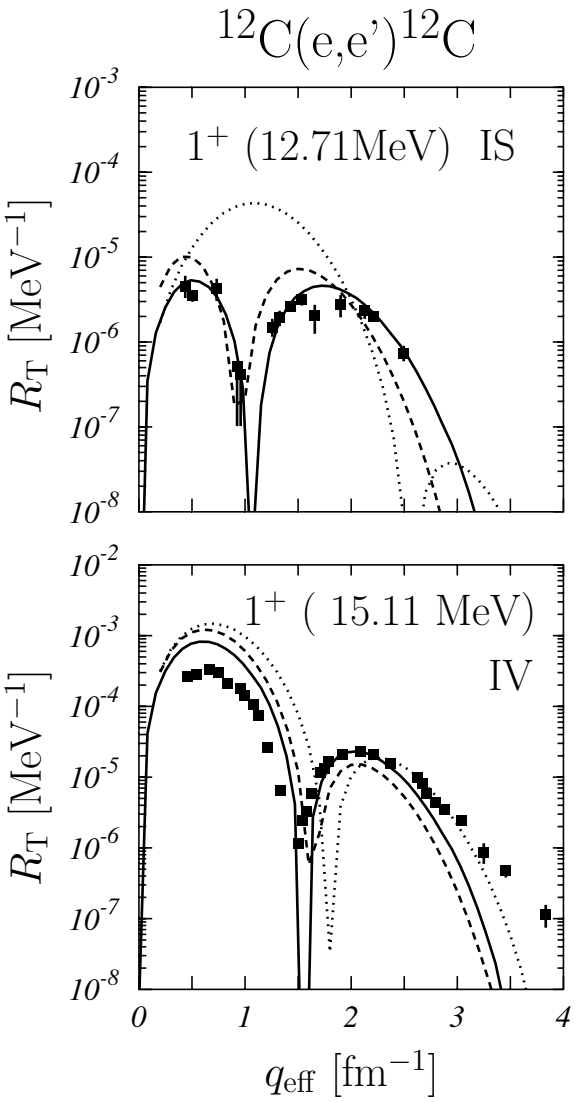

Figure 11: Electromagnetic responses of the 1^+ isospin doublet in ^{12}C. The full lines show the results of Fig. 2 obtained with the FR interaction. The dotted lines have been obtained with the D1 interaction but using the set of single particle wave functions and energies used in the phenomenological approach. The dashed lines are the results a self-consistent calculation with the D1 interaction. This means that the single particle basis has been generated by a Hartree-Fock calculation with the D1 interaction. The dotted and dashed curves in the IS panel have been otained by using the RPA amplitudes of the higher energy 1^+ solution. The lower energy amplitudes have been used to generate the curves shown in the IV panel.

Figure 12: Electromagnetic responses of some 4^- isospin doublets. The meaning of the lines is the same as in Fig. 11. Also in this case the low energy D1 responses are plotted together with the high energy phenomenological responses, and viceversa.

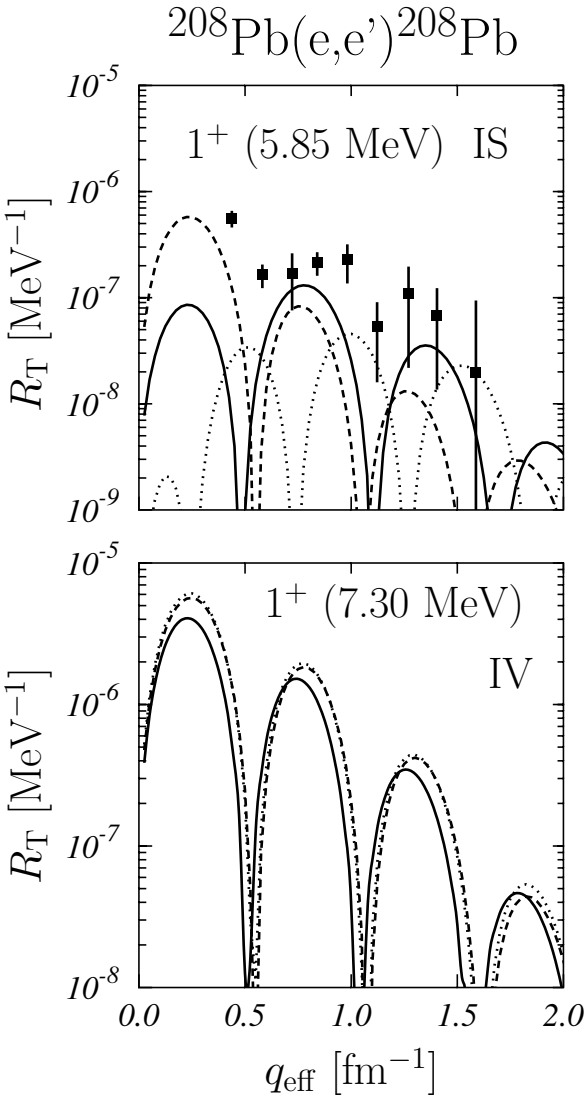

Figure 13: The same as Fig. 11 for the 1^+ isospin doublet in ^{208}Pb .